Astronomical and Astrophysical Transactions (*AApTr*), 2018, Vol. 30, Issue 4, pp. 367–378,
ISSN 1055-6796, Photocopying permitted by license only, ©Cambridge Scientific Publishers

Spectral characteristics of the AGNs Type 1 in UV/optical band

J. Kovačević-Dojčinović*, L. Č. Popović

Astronomical Observatory, Volgina 7, P.O. Box 74, 11160 Belgrade, Serbia

Received 10 October, 2016

Here we give a review of recent investigations of Active Galactic Nucleus (AGN) spectral characteristics in the UV and optical spectral band. The new model of Balmer continuum, and optical and UV Fe II templates are presented. We investigated the kinematical connections between UV and optical emission lines, and we try to locate the UV and optical Fe II emission region in AGN structure. The correlations between emission lines and continuum, as well as correlations found in Boroson and Green (1992), are analyzed in order to understand their physical origin. We explore possible the starburst connection to the AGN spectrum. Also, we investigate whether virial assumption is correct for the Hβ and Mg II emission lines in AGN spectra.

Keywords: Quasars: emission lines – galaxies: starburst – quasars: supermassive black holes

1 Introduction

Around 10% of all galaxies show very strong activity in the central part. The emission from the center of these galaxies has non-stellar origin and spectra are reach with strong emission lines. These objects are classified as Active Galactic Nuclei (AGNs). An AGN is very compact, so cannot be resolved by the largest telescope, even in the case of the closest galaxies. Therefore, spectroscopy is a unique tool to investigate the nature of AGNs. An AGN consists of a supermassive black hole surrounded by an accretion disk. The accretion disk is surrounded by gaseous regions, photoionized by a large amount of high energetic photons which are produced in process of accretion around super-massive black hole (see Peterson 2003). The photoionized gas closer to the accretion disk is called the Broad Line Region (BLR), because it produces the broad emission lines ($\sim$4000 km/s) that can be detected in AGN spectra. The narrow emission lines ($\sim$300 km/s) are produced in the emission region further from the black hole, called the Narrow Line Region (NLR).

The spectra of AGNs are very complex and showing different spectral features. In the case of AGNs type 1, there is strong continuum emission, and numerous broad

*Email: jkovacevic@aob.bg.ac.rs

and narrow emission lines. The continuum emission is composed of the power-law continuum which is coming from accretion disk and Balmer pseudocontinuum and pseudocontinuum of numerous iron lines. Some of the difficulties in spectral decomposition are modeling of the complex shapes of the broad emission lines and deblending of the lines which overlap each other. Therefore, the modeling of the Balmer continuum, which superposes to power-law continuum, and UV and optical Fe II spectral features, which overlap with other emission lines, is uncertain and represents problem in spectral decomposition.

The spectral decomposition is even more challenging if we take into account that there is a contribution of the host galaxy emission (radiation from stars), and possible starburst emission, which superposes with an AGN spectrum. The contribution from the host galaxy becomes significant comparing the pure AGN spectrum in the case of the low-luminosity AGNs, and must be taken into account (see e.g. Yip et al. 2004). On the other hand, the presence and contribution of the starburst emission in AGN spectra is more difficult to be determined.

To investigate the geometry, physics and kinematics of the AGN emission regions, one needs to remove the host galaxy contribution, and then to decompose the AGN spectrum, in order to obtain continuum and line components. Efforts have been made to investigate the correlations between different spectral properties and to determine the physics that is behind the detected correlations (for review see Kovačević-Dojčinović and Popović 2015).

Boroson and Green (1992) (hereafter BG92) have established the set of correlations between spectral properties, which are projected in eigenvector 1 (EV 1) in their principal component analysis. These correlations are specially interesting because their physical origin is still an open question. The optical Fe II emission lines are part of unexplained BG92 EV1 correlations. These lines are also interesting because of complex shape and difficulty in modeling, and there are several open questions about them: location of their emission region in the AGN structure, mechanisms of their excitation and their connections with UV Fe II emission (see review in Kovačević et al. 2010, Kovačević-Dojčinović and Popović 2015).

On the other hand, the starburst presence nearby AGN, observed in some objects (see Popović et al. 2009), may be one phase in AGN evolution. Namely, it is possible that an AGN in the earlier activity phase is composed of a starburst and a central engine (pure AGN) (see Marziani et al. 2003, Grupe 2004, Wang et al. 2006). In this scenario, one can expect that, besides the AGN emission, an additional significant starburst contribution can be present in the narrow lines and continuum emission.

For AGN type 1, the most appropriate methods for black hole mass estimation are those which use the strong broad emission lines (for review see Peterson et al. 2004). The basic assumption of these methods is that the BLR gas is virialized, i.e. that the main broadening mechanism of the broad emission lines is the Keplerian motion of gas around the super-massive black hole. However, the complex shapes of broad emission lines, with strong asymmetries in the line wings, imply that BLR is probably stratified, with complex kinematics (Popović et al. 2004). This implies that the assumption that some broad lines can be used as virial estimators must be checked.

In conclusion, to investigate the nature of AGNs, one has to model their spectra very carefully. Here we give an overview of the decomposition of AGN spectra in

the UV/optical spectral band. We present Balmer continuum model, and optical and UV Fe II templates (Section 2). In Section 3 we analyze the kinematical connections between UV and optical emission lines and the correlations found in BG92. We explore possible influence of starburst presence on AGN spectral properties in Section 4. In Section 5 we investigate whether virial assumption is correct for the Hβ and Mg II emission lines in AGN spectra. Finally, in Section 6 we summarize the results and give an outline of the proposal for the future work.

2 Modeling the UV and optical spectra

In order to analyze the UV and optical AGN spectral properties, one needs to decompose spectral features and to obtain the emission which is coming from different emission regions. For that purpose, we made a model of the continuum and line decomposition. Here we present the Balmer continuum model, and optical and UV Fe II templates.

2.1 Balmer continuum

The decomposition of the AGN continuum emission in the UV and optical band is complex, because it is composed of power-law emission, which arises in the accretion disk, and pseudocontinuum, which is the sum of the Balmer continuum and iron features. Our model of the Balmer continuum consists of the function given in Grandi (1982) for the Balmer continuum, in the case of a partially optically thick cloud, but with one degree of freedom less: for the intensity of the Balmer continuum, which is calculated using the prominent Balmer lines in an AGN spectrum. In this way, the less uncertain estimation of the Balmer continuum is achieved.

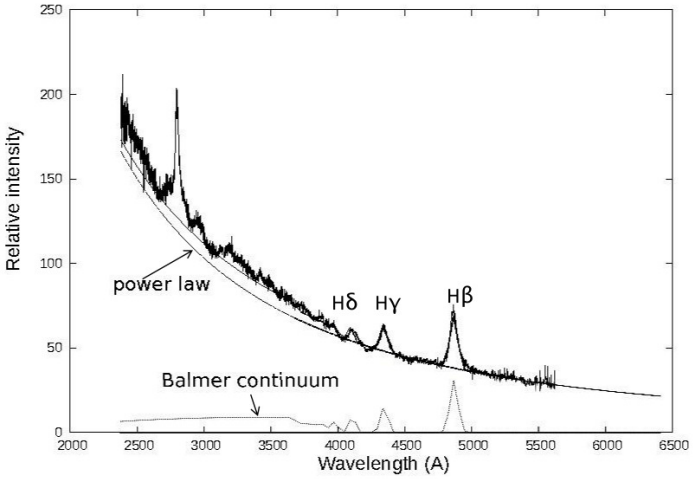


Figure 1 The model of continuum decomposition (SDSS J153301.60+194351.9). The Fe II lines and all narrow lines are previously removed from the spectrum.

We use the fact that the Balmer continuum intensity at the Balmer edge (λ = 3646 Å) is equal to the sum of intensities of all high order Balmer lines at the same wavelength. The broad component of each Balmer line is roughly described with only one Gaussian, which has the same width and shift for all Balmer lines, and their relative intensities are taken from the literature or calculated (see Kovačević et al. 2014).

Then, if the width, shift, and intensity of only one broad Balmer line (e.g. Hβ) are obtained from the fit, the sum of the fluxes of all high-order Balmer lines that contribute to the Balmer edge can be calculated, and we can obtain the intensity of the Balmer continuum at the Balmer edge.

The model is applied for the uniform temperature T_e = 15 000 K and optical depth at the Balmer edge fixed at $\tau_{BC} = 1$.

The model of continuum decomposition is shown in Fig. 1 and described in more detail in Kovačević et al. (2014).

2.2 Modeling the emission lines

In order to fit the emission lines we apply multi-Gaussian model, where each Gaussian represents emission from one kinematically different region, so the width and shift of each Gaussian reflect the kinematical properties of that region (Popović et al. 2004).

We model the emission lines in the spectral range of $\lambda\lambda$4000–5600 Å in optical and $\lambda\lambda$2650–3050 Å in the UV band. The Hβ line is decomposed into three Gaussians – one which represents the emission from the Narrow Line Region (NLR component), and two which represent emission from the outer (Intermediate Line Region – ILR) and inner (Very Broad Line Region – VBLR) part of the BLR. We fix all narrow lines in spectra to have the same widths and shifts, because we expect that they arise in the same emission region (for details see Kovačević et al. 2010 and Kovačević-Dojčinović and Popović 2015). The strongest UV line in observed UV band is Mg II λ2800 Å which is fitted with two broad Gaussians, one which fits the core, and one which fits the line wings. The most challenging task is deblending the iron lines which overlap with the Hβ, [O III] $\lambda\lambda$4959, 5007 Å and Mg II lines. In order to fit the UV and optical iron lines, and to obtain deblended profiles of the mentioned lines, the iron templates must be applied. The Fe II ion is very complex and therefore, there are numerous transitions which result in a very complex Fe II spectrum. The Fe II lines overlap and form irregular features, and therefore it is very difficult to calculate or empirically measure the relative intensities of iron lines.

We set up the UV Fe II template within $\lambda\lambda$2650–3050 Å range (Popović et al. 2003). The UV Fe II lines are divided into four multiplets. Within one multiplet, the relative intensities of the lines are fixed using the line strength from NIST* Atomic Spectra Database. The lines are fitted with four parameters of the intensity for each multiplet and with one parameter for width and one for shift, since it is assumed that all UV Fe II lines are originating in the same emission region and consequently have the same Doppler width and shift (for details see Popović et al. 2003 and Kovačević-Dojčinović and Popović 2015). The UV Fe II template is shown in Fig. 2.

The optical Fe II template is set up using the strongest Fe II emission lines within the $\lambda\lambda$4000–5600 Å range (see Kovačević et al. 2010, Shapovalova et al. 2012).

*https://www.nist.gov/

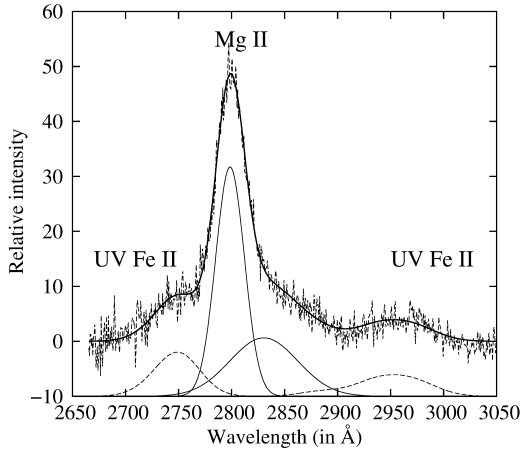


Figure 2 Decomposition of the UV spectrum in the wavelength range $\lambda\lambda$2650–3050 Å. The UV iron template is denoted with dashed line.

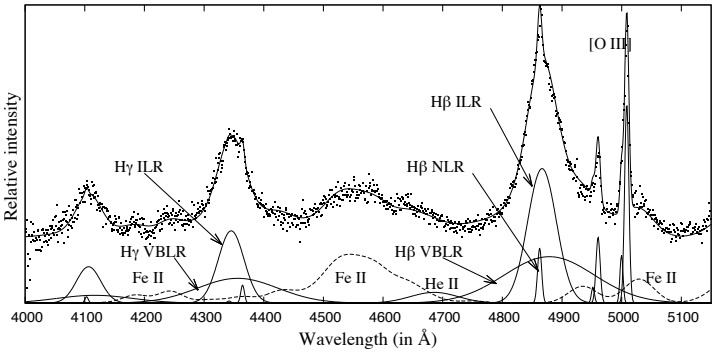


Figure 3 Decomposition of the optical spectrum in the wavelength range $\lambda\lambda$4000–5600 Å. The optical iron template is denoted with dashed line.

They are divided into five line groups according to the lower term of their transition. Relative intensities within each group are calculated with the formula described in Kovačević et al. 2010. However, ∼25% of optical Fe II emission cannot be explained with permitted lines for which the excitation energies are close to the lines of the five line groups. Therefore, their relative intensities are taken from well measured Fe II spectra of object I Zw 1. Finally, the optical Fe II template has 6 parameters of intensity for each line group, and three more parameters: for width, shift (we assume that all optical iron lines have the same widths and shifts) and temperature. This template is compared with other theoretical and empirical optical Fe II templates in the literature and we found that it can fit the optical Fe II lines more precisely than these templates (see Kovačević et al. 2010). The optical Fe II template is shown in Fig. 3 and is available online[†].

[†]The Fe II template $\lambda\lambda$4000–5600 Å, as well as the web application for fitting online, are given at http://servo.aob.rs/FeII_AGN/ as a part of Serbian Virtual Observatory.

3 The properties of the UV and optical iron lines

The construction of the UV and optical Fe II templates which can model very precisely the observed Fe II lines enables detailed investigation of the UV and optical Fe II properties, and their comparison. Using the large sample of objects obtained from Sloan Digital Sky Survey (SDSS), Data Release 7 (for selection criteria see Kovačević-Dojčinović and Popović 2015), we apply the spectral decomposition model (see the previous section) and try to investigate the connections between the spectral properties.

3.1 Comparison between kinematical properties

Analyzing the obtained kinematical parameters of the lines, we found that the widths of the UV Fe II, optical Fe II, ILR Hβ and Mg II core are in correlation, as well as their shifts. Since the widths and shifts of Gaussians represent kinematical properties of the emission regions, these results imply that emission regions of mentioned lines (or line components) are kinematicaly connected, i.e. that the UV and optical Fe II lines probably originate from the ILR. The average values of the widths of UV and optical Fe II lines are similar ($\sim$ 2500 km/s) but, there is a great difference in their average shifts. For optical Fe II lines the average shift is smaller than dispersion, while for UV Fe II it is: 1150 ± 580 km/s. This result can be explained as asymmetry of the UV Fe II emission region, while the optical Fe II emission region is probably symmetric (Kovačević-Dojčinović and Popović 2015).

3.2 The differences in correlations with other spectral lines

There is a significant difference between the optical Fe II and UV Fe II in their correlations with other spectral properties. The most important BG92 EV1 anticorrelations are between equivalent width (EW) of optical Fe II and Full Width at Halph Maximum (FWHM) of Hβ and between EW of optical Fe II and EW [O III]. The physical explanation of these correlations is still an open question. We measured a large set of spectral properties (Hβ, Hγ, Hδ, optical Fe II, UV Fe II, [O III] and Mg II lines) in order to check if there are similar correlations between some other lines in AGN spectra.

We found that the relationships of optical EW Fe II with EW [O III] and FWHM of broad lines (EV1 correlations) are exceptions, and we found no similar correlations between other emission lines. The only observed anticorrelation between line EWs is the one between the optical EW Fe II and EW [O III], while all other analyzed lines correlate with EWs of other lines or show no correlations (see Table 6 in Kovačević-Dojčinović and Popović 2015). Also, the EWs of analyzed lines increase as their widths increase, or there is no any correlation between their EWs and widths. Only in the case of the optical Fe II, their EW increases as the width decreases, i.e. the optical Fe II lines are stronger as they are narrower. In addition, while EWs of the other broad lines do not depend on widths of the other lines, the EW of the optical Fe II is stronger as broad lines are narrower (Mg II, Balmer lines).

One possible explanation of these peculiar correlations of the optical Fe II lines can be presence of starburst regions (see the next section) which can affect the emission of optical Fe II.

On the other hand, the UV Fe II lines do not show any of these peculiar correlations as the optical Fe II. Also, between the EWs of the optical and UV Fe II lines there is no correlation, and their flux ratio depends on different physical parameters, such as column density and microturbulence (see Joly 1987, Verner et al. 2004, Sameshima et al. 2011).

The differences between the correlations of optical and UV Fe II lines with some spectral properties can be caused by different mechanisms of their excitation.

4 The starburst contribution to AGN spectra

Commonly used diagnostics for distinguishing between objects with dominant AGN emission and those with dominant starburst emission in narrow emission lines is BPT diagram (Baldwin, Philips and Therlevich 1981). In this diagram, the objects are divided into subgroups using the fact that the AGN central engine and hot, young stars (in starburst regions) radiate different shapes of the ionizing continuum. Consequently, the flux ratios of narrow lines which are photoionized by AGN continuum are different from those photoionized by the continuum of young stars.

The construction of the BPT diagram for type 1 AGNs, where the permitted lines are composed of two or more components, is a very difficult task. The narrow components of the permitted lines (Hβ and Hα) must be extracted well, which is specially difficult for Narrow Line Seyfert 1 (NLSy1) galaxies[‡].

To explore the influence of starbursts to spectral correlations, the sample of 302 AGNs type 1 have been used, chosen from SDSS, Data Release 7 (for the selection criteria see Kovačević et al. 2010), and all emission lines in spectra are fitted with multi-Gaussian model (see Section 2).

Since we had complete measurements for the whole sample only for the narrow Hβ and [O III] lines, we accepted a ratio of $R = \log([\mathrm{O\ III}]/\mathrm{H}\beta_{NLR})$ (one axis of BPT diagram) as an indicator of the predominant AGN/starburst emission to the narrow emission lines (Popović and Kovačević 2011). We divided our sample into two subsamples: $R < 0.5$ (composite objects, hereafter starburst dominant) and $R > 0.5$ (pure AGNs, hereafter AGN dominant). Note that we found 91 objects from our sample of AGN type 1, to belong to starburst dominant group.

We investigated the correlations between different spectral properties and compared them in two subsamples – AGN dominant and SB dominant. It was found that correlations between spectral properties are different within these two subsamples. The most significant difference is seen for correlations between line widths and luminosities, and for BG92 EV1 correlations. Namely, in the starburst dominant subsample, the widths of narrow and broad emission lines are in high correlation with continuum luminosity (narrow lines: $r = 0.71$, $P = 0$, broad lines: $r = 0.79$, $P = 0$), while there is no correlations between widths and luminosities for AGN subsample (Popović and Kovačević 2011). These correlations are shown in Figs 4 and 5.

[‡]The subclass of AGNs with FWHM of broad Hβ component <2000 km/s, and ratio of [OIII]/Hβ_{total} <3.

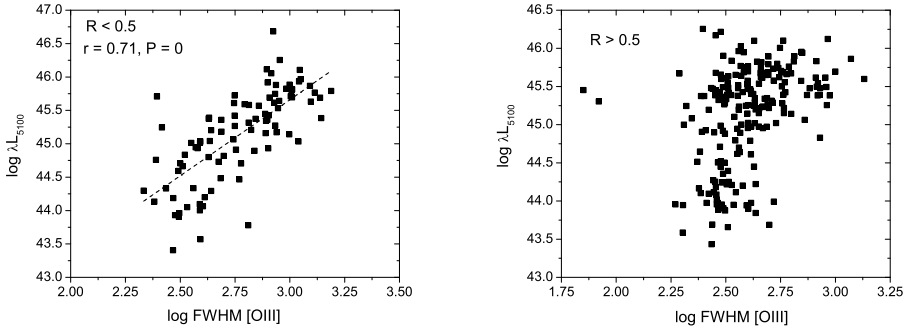


Figure 4 The relationship between the narrow lines width and continuum luminosity for starburst dominant ($R < 0.5$) and for AGN dominant ($R > 0.5$) subsample.

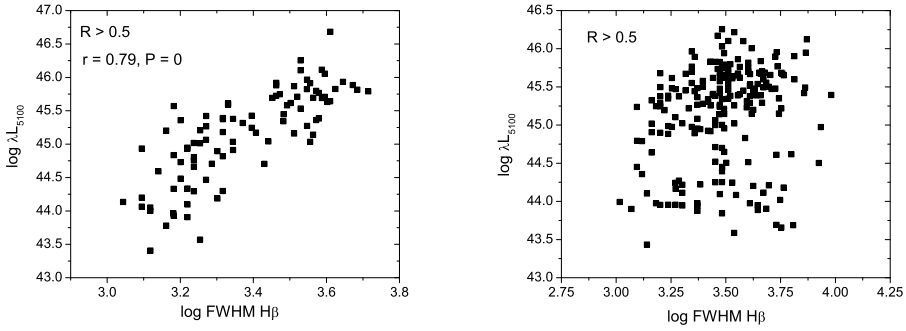


Figure 5 The relationship between the FWHM of the broad Hβ and continuum luminosity for starburst dominant ($R < 0.5$) and for AGN dominant ($R > 0.5$) subsample.

The good correlations between the line widths and luminosity in the composite AGNs may indicate that the broad component is not primarily a function of the rotation caused by the gravitational force, but rather by a random motion of the gas caused by different effects (such as the gas being randomly accelerated in several bursts). In such a case, part of the flux of the broad Balmer emission lines may arise in the stellar envelopes of Wolf-Rayet and OB stars associated with multiple SN events (Izotov et al. 2007). This must be taken into account while using the broad emission lines as virial estimators for black hole mass calculation (Popović and Kovačević 2011).

Well known anti-correlation of EW Fe II and FWHM Hβ, which is part of the BG92 EV1 correlations (see Section 3.2), as well as anti-correlation between EW Fe II and EW [O III], are stronger in AGN dominant subsample comparing SB dominant (Popović and Kovačević 2011). This may be caused by different physics in these two groups of objects, but also, distributions of the EW Fe II optical, EW [O III] and FWHM Hβ are narrower for the starburst dominant subsample comparing the AGN dominant, which may affect the strength of correlations as well. The SB dominant subsample, on average, has larger optical EW Fe II, smaller EWs of [O III], and smaller FWHMs of the broad lines, comparing the AGN dominant (Kovačević-Dojčinović and Popović 2015).

The large average values of the EW Fe II, and small values of EW [O III] and FWHM Hβ in the SB subsample comparing the AGN subsample may be explained by physical conditions caused by presence of starburst (Kovačević-Dojčinović and Popović 2015). Namely, as the column density increases due to the starburst presence, the flux of the optical Fe II increases, but the flux of the forbidden [O III] lines decreases, because of the collisional suppression or the weak ionizing continuum from starbursts. On the other hand, the starburst presence may be connected with early phase in the AGN evolution (see Sani et al. 2010). In that case, small average values of FWHM Hβ may be explained as generally smaller widths of the broad lines in young AGNs, because the Broad Line Region is not developed yet (Lípari and Therlevich 2006).

5 The virialization of the broad line region

Since broad lines in AGN spectra in some cases have complex shapes, it is necessary to investigate whether virial assumption is correct for all broad emission lines in AGN spectra, and is it valid in general for all AGN population. The lines which are the most frequently used as virial estimators are Hβ and Mg II.

In order to investigate the virialization of the BLR we analyzed the Hβ and Mg II line widths at 5%, 10% and 50% of the intensity maximum ($I_{\max}$) and corresponding shifts of their centroids with respect to the broad line peak, i.e. intrinsic redshifts (see Fig. 2 in Jonić et al. 2016). The starting hypothesis was that if there is a dominant Keplerian motion affecting the line widths, there should exist the gravitational redshift in the line profile (see Zheng and Sulentic 1990, Popović et al. 1995, Kollatschny 2003). We use the statistics of the large AGN sample to check the relationships between the widths and the shifts within the lines. The sample is chosen to have only red asymmetry in the Hβ and Mg II lines (for details see Jonić et al. 2016), because we assume that in line profiles with the blue asymmetry some other effects, as e.g. outflows, could be more dominant than the gravitational influence, so they are not convenient for this research.

For the broad Hβ line, we found good correlations between all measured intrinsic shifts and widths (at 50%, 10% and 5% of $I_{\max}$). Also, the theoretically expected relationship $\Delta z_{50} \sim FWHM^2$ (Jonić et al. 2016), where Δz_{50} is the intrinsic redshift at 50% of ($I_{\max}$), is confirmed, within the error-bars. The same relationship is confirmed for widths and corresponding intrinsic redshifts measured at different intensity levels (10% and 5% of $I_{\max}$). This implies that Hβ is a good virial estimator of AGN BH masses, and that the intrinsic redshift of the Hβ line is dominantly caused by gravitational effects.

In the case of the Mg II line, there is a correlation between the intrinsic redshift and width but only at 50% of $I_{\max}$. The theoretically expected relationship $\Delta z_{50} \sim FWHM^2$ is confirmed as well, but it failed for widths and intrinsic redshifts at 10% and 5% of $I_{\max}$. These results imply that the Mg II line can be used as a virial estimator only at 50% of $I_{\max}$, but the widths and shifts measured in wings of these lines cannot be used for this purpose.

6 Summary

Here we present the recent investigations of AGN spectral characteristics in the UV and optical spectral band. The new models of Balmer continuum and UV and optical Fe II templates are proposed. The correlations between different spectral properties are analyzed, in order to understand the kinematics and physics of the emission regions. The possible influence of the starbursts to AGN spectra is explored, as well as the virialization of the broad line region. We can summarize our results as follows:

- our models of the Balmer continuum emission and UV and optical Fe II templates enable more precise spectral decomposition of AGN spectra and improve the fitting procedure.
- the UV and optical Fe II lines probably originate from the same region in AGN structure – ILR, where the Mg II core and Hβ ILR component arise.
- there is a significant difference between the optical Fe II and UV Fe II in their correlations with other spectral properties. Among several observed emission lines, only EWs of the optical Fe II and [O III] anticorrelate, and only in the case of the optical Fe II lines, their EW tend to increase as broad lines in spectra are narrower.
- the correlations between spectral properties are different in the pure AGN subsample comparing starburst dominant subsample (with starburst presence nearby AGN). In the starburst dominant subsample, on average, EWs of optical Fe II are larger, EW [O III] smaller and FWHM Hβ are smaller, comparing the pure AGN subsample. This can be explained as influence of SB presence, which may be connected with an early phase in AGN evolution.
- The broad Hβ line, without blue asymmetry, seems to be a good virial estimator, which can be used for black hole mass estimation. On the other hand, when using the Mg II line as virial estimator, one needs to be more careful, since it is possible that in the Mg II wings, some other effects except gravity, are present (e.g. outflows).

For future work we propose investigation of starburst influence to unexplained correlations between optical spectral properties, using IR spectra for diagnostics of the starburst presence.

Acknowledgements This investigation is supported by the Ministry of Education, Science and Technological Development of Republic of Serbia in the frame of Project 176001 *Astrophysical spectroscopy of extragalactic objects.*

References

Baldwin, J. A., Phillips, M. M., Terlevich, R. (1981) PASP, 93, 5
Boroson, T.A., Green, R.F. (1992) ApJS 80, 109
Grandi, S. A. (1982) ApJ 255, 25
Grupe D. (2004) AJ 127, 1799
Izotov, Y.I., Thuan, T.X., Guseva, N.G. (2007) ApJ 671, 1297

Joly, M. 1987 A&A 184, 33
Jonić, S., Kovačević-Dojčinović, J., Ilić, D., Popović, L. Č. (2016) Ap&SS 361, 101
Kollatschny, W. (2003) A&A 412, 61
Kovačević, J., Popović, L. Č., Dimitrijević, M.S. (2010) ApJS 189, 15
Kovačević, J., Popović, L. Č., Kollatschny, W. (2014) AdSpR 54, 1347-1354
Kovačević-Dojčinović, J., Popović, L. Č. (2015) ApJS 221, 35
Lípari, S.L., Terlevich, R.J. (2006) MNRAS 368, 1001
Marziani, P. Zamanov, R. K., Sulentic, J. W., Calvani, M. (2003) MNRAS 345, 1133
Peterson, B.M. (2003) An Introduction to Active Galactic Nuclei, The University Press, Cambridge
Peterson, B.M., Ferrarese, L., Gilbert, K. M., Kaspi, S. et al. (2004) ApJ 613, 682
Popović, L. Č., Kovačević, J. (2011) ApJ 738, 68
Popović, L. Č., Mediavilla, E., Bon, E., Ilić, D. (2004) A&A 423, 909
Popović, L. Č., Mediavilla, E. G., Bon, E., Stanić, N., Kubičela, A. (2003) ApJ 599, 185
Popović, L. Č., Smirnova, A., Kovačević, J., Moiseev, A., Afanasiev, V. (2009) AJ 137, 3548
Popović, L. Č., Vince, I., Atanacković-Vukmanović, O., Kubičela, A. (1995) A&A 293, 309
Sameshima, H., Kawara, K., Matsuoka, Y., Oyabu, S., Asami, N., Ienaka, N. (2011) MNRAS 410, 1018
Sani, E., Lutz, D., Risaliti, G., Netzer, H., Gallo, L. C., Trakhtenbrot, B., Sturm, E., Boller, T. (2010) MNRAS 403, 1246
Shapovalova, A. I., Popović, L. Č., Burenkov, A. N. et al. (2012) ApJS 202, 10
Verner, E., Bruhweiler, F., Verner, D., Johansson, S., Kallman, T., Gull, T. (2004) ApJ 611, 780
Wang, J., Wei, J. Y., He, X. T. (2006) ApJ 638, 106
Yip, C. W., Connolly, A. J., Vanden Berk, D. E., Ma, Z., Frieman, J. A., et al. (2004) AJ 128, 2603
Zheng, W., Sulentic, J. W. (1990) ApJ 350, 512